Journal of Sustainability Science and Management
Volume 19 Number 11, November 2024: 15-38
eISSN: 2672-7226

MARINE NATURAL PRODUCTS AS POTENTIAL INHIBITORS AGAINST PATHOGENIC *Streptococcus agalactiae* USING MOLECULAR DOCKING STUDY FOR HUMAN AND FISH DISEASE CONTROL

WEE YE ZHI[1], SAIRATUL DAHLIANIS ISHAK[2,3] AND SITI AISYAH RAZALI[1,4]*

[1]Faculty of Science and Marine Environment, Universiti Malaysia Terengganu, 21030 Kuala Nerus, Terengganu, Malaysia. [2]Higher Institution Centre of Excellence, Institute of Tropical Aquaculture and Fisheries, Universiti Malaysia Terengganu, 21030 Kuala Nerus, Terengganu, Malaysia. [3]Food Security Research Cluster, Universiti Malaysia Terengganu, 21030 Kuala Nerus, Terengganu, Malaysia. [4]Biological Security and Sustainability Research Interest Group, Universiti Malaysia Terengganu, 21030 Kuala Nerus, Terengganu, Malaysia.

**Corresponding author: aisyarazali@umt.edu.my*
http://doi.org/10.46754/jssm.2024.11.002
Received: 13 March 2024 *Accepted: 10 August 2024* *Published: 15 November 2024*

Abstract: *Streptococcus agalactiae* is a zoonotic bacterium infecting farmed and wild fish species, which damages the central nervous system and tissues. Doubtless, *S. agalactiae* infection not only adversely impacts the development of the aquaculture and fishing industry but also endangers the public's health. It severely compromises human immunity when raw or undercooked infected fish are consumed. To date, *S. agalactiae* is multidrug resistant to six widely-used antibiotics: Ampicillin, norfloxacin, aminoglycosides, fluoroquinolone, sulfamethoxazole, and tetracycline. Therefore, the study aims to investigate the potentiality of Marine Natural Products (MNPs) as inhibitors targeting *S. agalactiae* phosphopentomutase receptor, which is involved in the biosynthesis process of bacterial nucleic acid. Molecular docking analysis, which tested eight MNPs from the Comprehensive Marine Natural Product Database (CMNPD), revealed CMNPD30307, CMNPD30309, and CMNPD30310 as promising antibiotics. These MNPs, adhering to Lipinski's rule with low binding energy, high gastrointestinal absorption, and high bioavailability scores exhibit potential for further in vitro and in vivo analysis. Nevertheless, given the escalating concerns surrounding biodiversity loss and over-exploitation of marine resources, it is crucial to adopt a sustainable approach in the extraction, collection, and utilisation of these MNPs to contribute to the sustainable and ethical conduct of research in the field of bioprospecting.

Keywords: Aquatic health management, computer-aided drug design, food-borne disease, antibiotic resistance, zoonotic.

Introduction

Streptococcus agalactiae also known as Group B Streptococcus (GBS) is a highly pathogenic Gram-positive bacterium (Joyce & Doran, 2023). *S. agalactiae* with sequence type ST283 is a zoonotic clone of GBS that has severely infected farmed freshwater fish, particularly tilapia (*Oreochromis* sp.) (Syuhada *et al*., 2020; Phuoc *et al*., 2021; Schar *et al*., 2023). A huge epidemic of *S. agalactiae* infection was reported in 2015 where Singaporean adults were severely infected with *S. agalactiae* infection with the sequence type of ST283 after they consumed raw freshwater fish that was infected with *S. agalactiae* (ST283) (Favero *et al*., 2020). Among the examples of health problems that are associated with *S. agalactiae* include neonatal infection (Silva & Winkelströter, 2019), Urinary Tract Infection (UTI) among pregnant women (Desai *et al*., 2021), bacteremia among elderly and immunocompromised individuals (Yoshida *et al*., 2023), bone and joint infection (Lacasse *et al*., 2022), endocarditis (Saito *et al*., 2023), and meningitis (Tsalta-Mladenov *et al*., 2022). Deng *et al*. (2019) reported that a total of 28 antibiotic-resistant *S. agalactiae* isolates of serotype I and III were found in diseased farmed tilapia, Yayu (*Schizothorax prenanti*), and Yellow River striped fish (*Schizopygopsis*

pylzovi) in China, which eventually caused increased fish morbidity and mortality rates thereby resulting in major economic loss.

Generally, *S. agalactiae* colonises the GI tract of healthy adults without causing any harm, particularly in women (Abdullah *et al*., 2023). Nevertheless, *S. agalactiae* is an opportunistic pathogen whereby it has been regarded as a major contributor to severe newborn infections since 1970; thereby, contributing to high morbidity and death rates (Miselli *et al*., 2022). In the case of severe neonatal infection, neonates below seven days of age often experience early-onset neonatal septicemia (Aldana-Valenzuela *et al*., 2019) as well as meningitis with mortality rates up to 60% after colonisation of maternal *S. agalactiae*. Two recently reported cases of human sepsis caused by *S. agalactiae* (ST283) fish-related infection were the first human cases from Malaysia (Zohari *et al*., 2023). Therefore, these phenomena eventually signal an immediate urgency and the need for scientists to manufacture as many effective drugs as possible to cure and eliminate the deadly bacterial infection.

Phosphopentomutase has been identified as a promising drug target for *S. agalactiae* due to its high druggability score and crucial role in bacterial metabolism and virulence (Favero *et al*., 2020). This enzyme is essential for synthesising nucleic acid biosynthesis and producing metabolic energy in *S. agalactiae* (Doello *et al*., 2022; Giesen *et al*., 2023). Previous studies have demonstrated that inhibition of bacterial phosphopentomutase can lead to bacterial lysis, agglutination, and ultimately cell death (Osowole *et al*., 2017). These findings highlight the potential of targeting phosphopentomutase to develop new antibacterial agents against *S. agalactiae.*

Marine Natural Products (MNPs) have emerged as promising candidates for antibiotic development due to their structural similarity to animal metabolites and potent antibacterial properties (Kazmi *et al*., 2019). MNPs have been shown to disrupt bacterial biofilms and crucial metabolic processes (Deng *et al*., 2022). Kong *et al*. (2018) investigated eight MNPs (CMNPD30307-CMNPD30314) derived from the marine fungus *Aspergillus fumigatus* HNMF0047. These compounds, classified as helvolic acid derivatives and triterpenoids were characterised using various spectroscopic methods. Notably, helvolic acid and two of its derivatives (CMNPD30311 and CMNPD30312) exhibited potent antibacterial effects against *S. agalactiae* with minimum inhibitory concentration (MIC) values of 8, 16, and 2 μg mL^{-1}, respectively.

Helvolic acid, a fusidane-type antibiotic has gained attention due to its exceptional biological activity and lack of cross-resistance to commonly used antibiotics (Lv *et al*., 2017). As a bacteriostatic agent, helvolic acid primarily inhibits the translocation step of bacterial protein synthesis, showing particular efficacy against Gram-positive bacteria (Hussein *et al*., 2022). The current computational study aims to investigate the potential of these MNPs as inhibitors of *S. agalactiae* phosphopentomutase to disrupt nucleic acid biosynthesis and energy production in the bacteria. This research leverages the Comprehensive Marine Natural Product Database (CMNPD) developed by Lyu *et al*. (2021) to explore novel therapeutic strategies against *S. agalactiae* infections.

Materials and Methods

Sequence-based Analysis

Multiple Sequence Alignment (MSA)

The target sequence of *S. agalactiae* phosphopentomutase was retrieved from UniProt (The UniProt Consortium, 2019) under the accession number Q8CMH7. BLASTp was performed to select three homologues of the bacterial protein with the highest percentage of query cover and identity. MSA between *S. agalactiae* phosphopentomutase and its homologues was later performed by using Clustal Omega (Sievers *et al*., 2011) and visualised using ESpript3 (Robert & Gouet, 2014) to find out the aligned conserved regions predicted by the external NCBI Conserved Domain Search.

Physicochemical Characterisation

Physicochemical properties of *S. agalactiae* phosphopentomutase such as its amino acid composition, amino acid count, molecular weight, theoretical pI, Grand Average of Hydropathicity (GRAVY) value, number of negatively charged and positively charged residues, aliphatic index, and instability index were measured and analysed by using Expasy ProtParam Tool (Walker, 2005).

Structure-based Analysis

Model Construction and Structure Analysis

Homology modelling was performed by using AlphaFold2 software (Jumper *et al*., 2021) embedded in UCSF ChimeraX (Pettersen *et al*., 2021) to model the 3D crystal structure of *S. agalactiae* phosphopentomutase. In this case, among the five different protein models being predicted by AlphaFold2, the best-predicted protein model was selected based on the highest value of the predicted Local Distance Difference Test (pLDDT) score first, followed by the expected Template Modelling (pTM) score. This is because the higher the value of the pLDDT score, the higher the confidence percentage of every amino acid residue of the predicted protein model. In addition, the higher the value of the pTM score (above 0.5), the higher the significance of the structural similarity between the target protein structure and its homologues (Jumper *et al*., 2021).

The topology of *S. agalactiae* phosphopentomutase was measured and investigated using PDBSum generated (Laskowski *et al*., 1997). This is to observe how the secondary structure folds in the three-dimensional space, namely alpha helices and beta-pleated strands of *S. agalactiae* phosphopentomutase. As a result, the potential binding sites flexibility and accessibility of *S. agalactiae* phosphopentomutase, the local environment around the binding sites as well as the preferred binding orientation and positioning of ligands within the binding sites can be investigated (Laskowski, 2022).

After 3D structure prediction has been performed, the 3D model structure of *S. agalactiae* phosphopentomutase was further evaluated by using SAVESv6.0 structure validation server tools, which include ERRAT (Colovos & Yeates, 1993), PROCHECK (Laskowski *et al*., 2006), WHATCHECK (Bhattacharya *et al*., 2007), VERIFY 3D (Eisenberg *et al*., 1997), and ProSA-web server (Wiederstein & Sippl, 2007). This was performed to ensure that the predicted protein model of *S. agalactiae* phosphopentomutase was accurate, reliable, and high quality before the model was further visualised by using protein visualisation tools such as ChimeraX (Version 1.6) (Pettersen *et al*., 2021) and Pymol (Version 2.5.4) (Yuan *et al*., 2017).

Protein-ligand Interaction

Binding Site Prediction

Before the site-specific docking process was performed, both the substrate binding sites and cofactor binding sites of *S. agalactiae* phosphopentomutase predicted by NCBI Conserved Domain Search were compared with the three protein's homologues derived from the previous literature review (Panosian *et al*., 2011) by performing structural alignment using UCSF Chimera. This is to precisely identify and verify all available active site residues of *S. agalactiae* phosphopentomutase.

To elaborate in more detail, a structural superimposition process was performed to align the structure of *S. agalactiae* phosphopentomutase (chain A only) with the structure of *Bacillus cereus* phosphopentomutase (PDB ID: 3UN2; chain A only). Secondly, a structural superimposition process was performed to align the structure of *S. agalactiae* phosphopentomutase (chain A only) with the structure of *Bacillus cereus* ATCC 14579 phosphopentomutase (PDB ID: 3M8Z; chain A only). Lastly, a structural superimposition process was performed to align the structure of *S. agalactiae* phosphopentomutase (chain A only) with the structure of *Streptococcus*

mutans phosphopentomutase (PDB ID: 3M7V; chain B only).

Protein and Ligand Preparation

S. agalactiae phosphopentomutase was first prepared by using AutoDockTools4 (Morris *et al*., 2009) and was embedded inside AutoDock4 (AD4) software (Version 1.5.7), whereby the files were later saved in the form of PDBQT format. In this case, there were several steps of protein preparation (Forli *et al*., 2016) which needed to be followed namely adding polar hydrogens, checking residues for missing atoms, adding Kollman charges, editing, and lastly, assigning AD4 type for all of the atoms within the protein structure (Morris *et al.*, 2009).

A list of eight MNPs with the compound identification number (CMNPD30307, CMNPD30308, CMNPD30309, CMNPD30310, CMNPD30311, CMNPD30312, CMNPD30313, and CMNPD30314) were retrieved and downloaded from the CMNPD as shown in Table 1.

The eight MNPs were prepared in the form of PDBQT format before being further tested as possible ligands to inhibit the function of *S. agalactiae* phosphopentomutase through a molecular docking approach. In this instance, the steps of ligand preparation which needed to be followed were assigning AD4 type for all of the atoms within the ligand structure, adding polar hydrogens, and adding Gasteiger charges to the ligand of interest (Morris *et al*., 2009).

Molecular Docking

The site-specific docking process was performed using AutoDock4, where *S. agalactiae* phosphopentomutase was first docked with two manganese ions cofactors, Mn^{2+}, before being docked with the eight MNPs of interest. A Grid Parameter File (GPF) was prepared for running AutoGrid and a Docking Parameter File (DPF) was ready for running AutoDock4 (Morris *et al*., 2009). The number of points in the x, y, and z dimensions was set at 50, 80, and 80, respectively while the x, y, and z centre of the grid box were set at 4.715, 4.665, and -8.147, respectively for every single docking process. The genetic algorithm was set at 30 to generate 30 different ligand conformations. Out of 30 different ligand conformations, the best conformation of the ligand with the lowest estimated free energy of binding was selected and downloaded in the form of PDB format (Asiamah *et al*., 2023).

Pharmacokinetic Assessment of MNPs

The pharmacokinetic properties of the eight MNPs were measured and evaluated by using a SwissADME server (Daina *et al*., 2017) in order to investigate whether they are suitable for human oral consumption in adherence to Lipinski's rule of five (Benet *et al*., 2016). Firstly, the selected MNP must have a Molecular Weight (MW) of less than 500 g/mol or 500 Da in molecular size (Waring, 2009) to make sure that the molecule is not too big to pass through the phospholipid membrane of enterocytes that are located within the GI tract of humans. Also, the selected MNP must possess a Polar Surface Area (PSA) of less than 140 angstrom^2 (Remko *et al*., 2014) and a hydrophobicity value (log P) of less than five to ensure that the molecule is polar and hydrophilic, so that the molecule can dissolve in water easily (Zuegg & Cooper, 2012). Furthermore, the selected MNP must acquire less than 10 hydrogen bond acceptors and less than five hydrogen bond donor groups (Zheng *et al*., 2017). Lastly, the selected MNP must also have less than 10 rotatable bonds (Caron *et al*., 2020) to ensure that the molecule is not too flexible until it encounters difficulty in adopting a proper conformation to pass through the phospholipid membrane of enterocytes. All in all, the selected MNPs will be orally active, where they can be safely consumed by humans orally, if and only if they follow Lipinski's rule of five.

Table 1: Eight different MNPs derived from CMNPD with its presented 2D structure, name, compound ID number, and molecular formula

2D Structure	Name	Compound ID Number	Molecular Formula
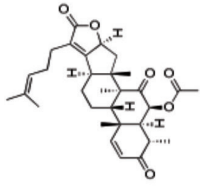	16-O-deacetylhelvolic acid 21,16-lactone	CMNPD30307	$C_{31}H_{40}O_6$
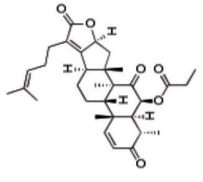	6-O-propionyl-6,16-O-dideacetylhelvolic acid 21,16-lactone	CMNPD30308	$C_{32}H_{42}O_6$
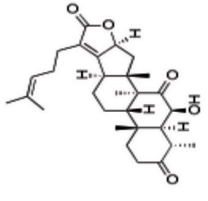	1,2-dihydro-6,16-O-dideacetylhelvolic acid 21,16-lactone	CMNPD30309	$C_{29}H_{40}O_5$
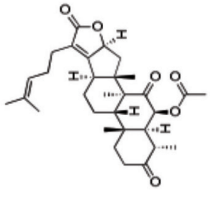	1,2-dihydro-16-O-deacetylhelvolic acid 21,16-lactone	CMNPD30310	$C_{31}H_{42}O_6$

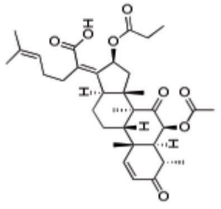	16-O-propionyl-16-O-deacetylhelvolic acid	CMNPD30311	$C_{34}H_{46}O_8$
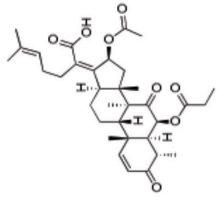	6-O-propionyl-6-O-deacetylhelvolic acid	CMNPD30312	$C_{34}H_{46}O_8$
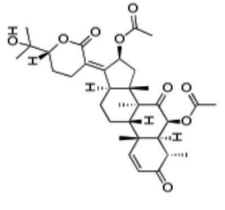	6ß,16ß-diacetoxy-25-hydroxy-3,7-dioxo-29-nordammara-1,17(20)-dien-21,24-lactone	CMNPD30313	$C_{33}H_{44}O_9$
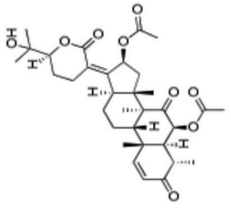	24-epi-6ß,16ß-diacetoxy-25-hydroxy-3,7-dioxo-29-nordammara-1,17(20)-diene-21,24-lactone	CMNPD30314	$C_{33}H_{44}O_9$

Results and Discussion

Sequence-based Analysis

Multiple Sequence Alignment (MSA)

BLASTp analysis of *S. agalactiae* phosphopentomutase identified three homologues with high query cover (99% to 100%) and identity (55.94% to 88.09%), which are *Streptococcus mutans* (PDB: 3M7V), *Bacillus cereus* ATCC 14579 (PDB: 3M8Z), and *Bacillus cereus* (PDB: 3UN2) (Table 2). Higher query cover and identity percentages indicate greater structural similarity between *S. agalactiae* phosphopentomutase and its homologues (Cicaloni *et al*., 2022), increasing the likelihood of accurately identifying conserved domains and binding sites. The extremely low e-values further support significant sequence similarity that is unlikely to occur by chance (Yang & Tung, 2006). These homologues were used to perform multiple sequence alignment using Clustal Omega.

NCBI Conserved Domain Search (Wang *et al*., 2023) predicted two active sites of the protein, which are the cofactor (Mn) binding site and the substrate binding site. The Mn binding site residues were identified as ASP-13, THR-92, ASP-165, ASP-298, HIS-303, ASP-339, HIS-340, and HIS-351 (Figure 1). The substrate binding site comprised 15 residues, which were identified as THR-92, SER-140, GLY-141, TYR-161, ASP-165, GLN-169, ARG-202, ILE-204, ARG-206, ARG-217, LYS-249, ASP-298, HIS-303, HIS-340, and HIS-351 as shown in Figure 2. Four conserved domains of the protein were identified: Metalloenzyme (pfam01676), deoB (TIGR01696), phosphopentomutase (PPM) (cd16009), and DeoB (COG1015). These domains are involved in metal binding and catalysis (Valasatava *et al*., 2018), purine and pyrimidine salvage pathways (Bizarro & Schuck, 2007), interconversion of ribose phosphates (Panosian *et al*., 2011), and carbohydrate transport and metabolism (McLeod *et al*., 2011), respectively.

The result of MSA between the target *S. agalactiae* phosphopentomutase and its three homologues with PDB IDs of 3M7V, 3M8Z, and 3UN2 is shown in Figure 2. MSA revealed high conservation among the homologues, with a notable substitution of THR-92 in *S. agalactiae*

Table 2: Three homologues of *S. agalactiae* phosphopentomutase generated by BLASTp with respective source of organisms, PDB ID, chain, percentage of query cover, percentage of identity, and e-value

Organism	PDB ID	Chain	Percentage of Query Cover (%)	Percentage of Identity (%)	e-value
Streptococcus mutans	3M7V	B	100	88.09	0.0
Bacillus cereus ATCC 14579	3M8Z	A	99	56.19	4e-159
Bacillus cereus	3UN2	A	99	55.94	3e-158

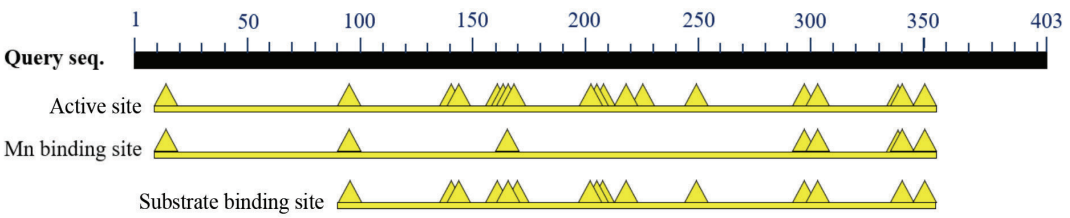

Figure 1: Protein graphic summary which demonstrates the active site residues of *S. agalactiae* phosphopentomutase predicted by NCBI Conserved Domain Search

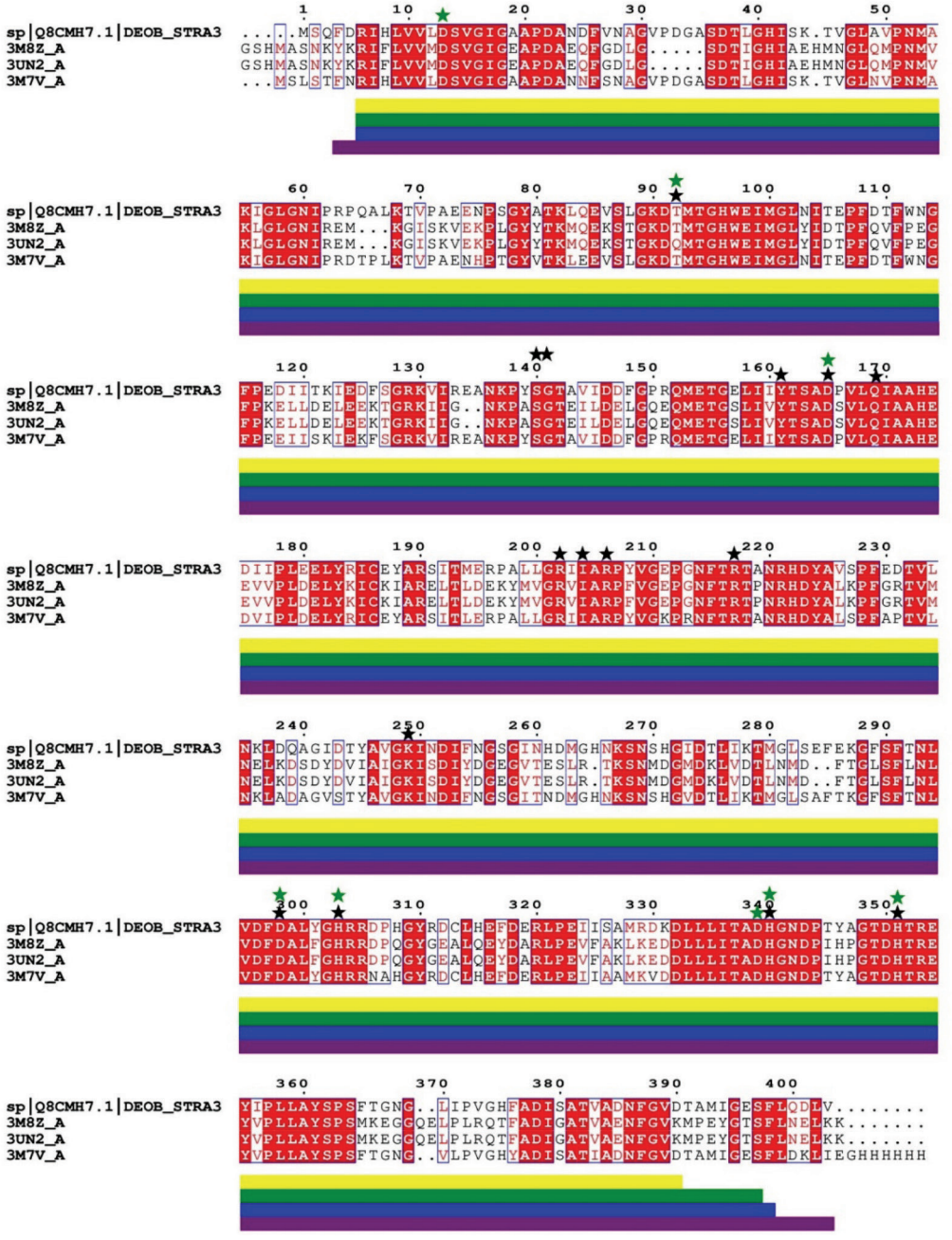

Figure 2: Illustration of MSA between *S. agalactiae* phosphopentomutase (Q8CMH7) and its three homologues (3M7V, 3M8Z, and 3UN2) performed by using Clustal Omega server and visualised by using ESpript 3 server. The black stars indicate all the substrate binding sites of *S. agalactiae* phosphopentomutase whereas the green stars indicate all the cofactor binding sites of two Mn ions. The yellow bar shows the location of the metalloenzyme domain; green bar shows the location of the deoB domain; blue bar shows the location of the phosphopentomutase (PPM) domain; and violet bar shows the location of the DeoB domain of the bacterial protein

by GLN-85 in *B. cereus* phosphopentomutase despite similar physicochemical properties.

Physicochemical Characterisation

The Expasy ProtParam Tool server was used to compare the physicochemical properties of Q8CMH7 (*S. agalactiae* phosphopentomutase) and its homologues 3M7V, 3M8Z, and 3UN2 as shown in Table 3. These proteins exhibit electrical neutrality at pH values ranging from 4.75 to 5.62, representing their theoretical isoelectric points (pI). This characteristic is crucial for understanding their behaviour in different pH environments: Below their pI, the proteins become positively charged and protonated while above it, they become negatively charged and deprotonated (Santhoshkumar & Yusuf, 2020; Ghosal *et al*., 2023). All four proteins are hydrophilic as indicated by their negative GRAVY (Grand Average of Hydropathicity) values, suggesting high water solubility. Furthermore, they tend to be negatively charged under physiological conditions due to having more negatively charged residues than positively charged ones (Chen, 2005).

The phosphopentomutase enzyme and its homologues demonstrate high thermal stability as evidenced by their aliphatic indices exceeding 80%. This indicates that over 80% of their structure consists of hydrophobic and non-polar amino acids such as alanine, valine, leucine, and isoleucine. The aliphatic index is directly correlated with the protein's thermal stability with higher values indicating greater stability at elevated temperatures (Panda & Chandra, 2012). All four proteins are also considered stable in vitro with instability indices below 40 (Xu *et al*., 2016). These physicochemical properties provide valuable insights into the proteins behaviour under various conditions and their potential interactions in biological systems.

Structure-based Analysis

Model Construction and Structure Analysis

The secondary structure and the best-predicted model of *S. agalactiae* phosphopentomutase (UniProt ID: Q8CMH7) were generated using PDBSum and AlphaFold2, respectively as shown in Figure 3. Based on the topological analysis in Figure 3 (a), it can be deduced that the secondary structure of phosphopentomutase

Table 3: Physicochemical properties comparison between Q8CMH7, 3M7V, 3M8Z, and 3UN2

Characteristics	Q8CMH7	3M7V	3M8Z	3UN2
No. of amino acid	403	413	399	399
Molecular weight (Da)	44,201.61	45,164.89	44,459.45	44,486.48
Theoretical pI	4.75	5.62	4.83	4.83
GRAVY value	-0.237	-0.221	-0.404	-0.411
No. of negatively charged residues (Asp + Glu)	59	51	66	66
No. of positively charged residues (Arg + Lys)	32	35	42	42
Total no. of atoms	6151	6304	6217	6220
Molecular formula	$C_{1965}H_{3036}N_{528}O_{610}S_{12}$	$C_{2013}H_{3118}N_{552}O_{610}S_{11}$	$C_{1973}H_{3095}N_{517}O_{614}S_{18}$	$C_{1974}H_{3096}N_{518}O_{614}S_{18}$
Aliphatic index	85.71	86.22	81.85	81.85
Instability index (stable < 40)	30.38	26.97	31.35	31.73

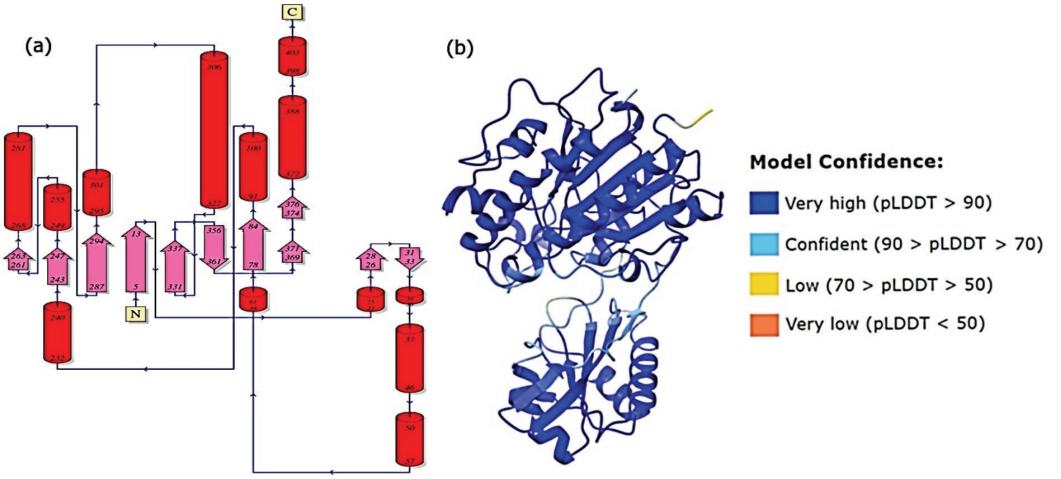

Figure 3: (a) The secondary structure of *S. agalactiae* phosphopentomutase enzyme generated by PDBSum and (b) the best predicted protein model of *S. agalactiae* phosphopentomutase by AlphaFold2 with the attached reference percentage of model confidence per residue

enzyme consists of three sheets, two beta alpha beta units, four beta hairpins, one psi loop, 16 strands, 17 helices, 15 helix-helix interacts, 29 beta turns, and four gamma turns (Laskowski, 2022).

The machine learning-based algorithm of AlphaFold2 software (Casadevall *et al*., 2023) generated the best-predicted protein model with the highest pLDDT score of 96.9 and the highest pTM score of 0.915 as shown in Figure 3 (b). It is important to note that the higher the pLDDT score of the protein model, the higher the average confidence score percentage per residue of the protein model itself (Jumper *et al.*, 2021). Also, the higher the pTM score of the protein model, the higher the percentage of the overall topological accuracy of the protein model predicted by AlphaFold2 (Jumper *et al.*, 2021).

Model Evaluation

The 3D structure of *S. agalactiae* phosphopentomutase enzyme (Q8CMH7) was evaluated using multiple tools: PROCHECK (Laskowski *et al*., 2006), Verify-3D (Eisenberg *et al*., 1997), ERRAT (Colovos & Yeates, 1993), WHATCHECK (Bhattacharya *et al*., 2007), and ProSA-web server (Wiederstein & Sippl, 2007). These tools assess different aspects of protein structure quality, providing a comprehensive evaluation.

PROCHECK analysis revealed excellent stereochemical quality with 100% of amino acid residues located in the allowed regions of the Ramachandran plot (88% in most favoured regions) as shown in the appendix (SF-1). The bond length or angle deviation of 3.8 (below the maximum of 4.2) and zero bad contacts between residues further support the high quality of the model (Reddy & Rao, 2020; Qaiser *et al*., 2021).

Verify-3D results showed that 84.37% of amino acid residues have an average 3D-1D score ≥ 0.1, exceeding the 80% threshold (SF-2). This indicates compatibility between the 3D structure and the primary sequence (Ugurel *et al*., 2020). ERRAT analysis yielded an overall quality factor of 95.641% (SF-3), surpassing the 95% threshold for high-resolution structures (Michael *et al*., 2023).

Based on Table 4, WHATCHECK results provided mixed insights. While the structure showed high atom packing quality and normal chi-1 or chi-2 rotamers, it indicated poor backbone conformation (Sobolev *et al*., 2020). Bond lengths and angles were slightly smaller than ideal, suggesting a somewhat tighter

structure (Ratnaningsih & Saepulloh, 2022). Omega dihedral angles and side chain planarity slightly differed from ideal values (Jha *et al*., 2022).

The ProSA-web server analysis yielded a Z-score of -10.37, indicating that the model falls within the score range for native proteins of similar size (SF-4). This suggests that the enzyme could be experimentally modelled using Nuclear Magnetic Resonance (NMR) methods (Pereira *et al*., 2021).

The summary of the 3D model evaluation for *S. agalactiae* phosphopentomutase enzyme is displayed and plotted in Table 5. In conclusion, the *S. agalactiae* phosphopentomutase enzyme model successfully passed all four major evaluation tests (PROCHECK, Verify-3D, ERRAT, and ProSA-web). While some aspects, particularly the backbone conformation may require further refinement, the overall quality of the model appears to be suitable for further structural and functional analyses.

Protein-ligand Interaction

Location and Binding of Mn Ions

Generally, phosphopentomutase enzyme has two Mn ions per subunit, which include a catalytic Mn ion (labelled as Mn-1) (Rigden *et al*., 2003) and a structural Mn ion (labelled as Mn-2) (Panosian *et al*., 2011) as shown in Figure 4. The catalytic Mn ion is found to be coordinated by four residues, which are ASP-165, ASP-298, HIS-303, and HIS-351, where the catalytic Mn ion functions to speed up the transfer of phosphate group from the first carbon (C1) of D-ribose-1-phosphate (RIP) to the fifth carbon (C5) position to convert RIP to D-ribose-5-phosphate (R5P). Whereas, the structural Mn ion is found to be coordinated by four residues, which are ASP-13, THR-92, ASP-

Table 4: Overall summary report of WHATCHECK result for the predicted phosphopentomutase enzyme

Structure Z-scores		**RMS Z-scores**	
Parameters	**Values**	**Parameters**	**Values**
First generation packing quality	-0.312	Bond lengths	0.58
Ramachandran plot appearance	-1.485	Bond angles	1.021
Chi-1 or chi-2 rotamer normality	1.054	Omega angle restraints	1.099
Backbone conformation	-29.107	Side chain planarity	1.538

Table 5: Summary of 3D model evaluation for *S. agalactiae* phosphopentomutase using different tools. NPS is native protein size check whether the Z-score of the input structure is within the range of scores for native proteins of similar size

Model Evaluation Tools	**Evaluation Scheme**	**Score (%)**	**Normal Range of the Score (%)**
PROCHECK	The number of residues in the allowed region based on Psi/Phi Ramachandran plot	100	> 90
VERIFY3D	The number of residues having an average 3D-1D score above 0.1	84.37	> 80
ERRAT	The overall quality for non-bonded atomic interaction	95.641	> 50
ProSA-web	Model evaluation by calculating an overall quality score (Z-score)	-10.37	NPS

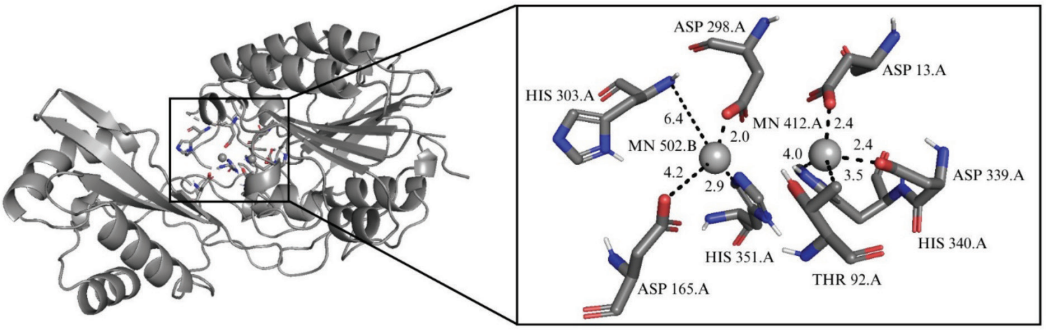

Figure 4: A complex of phosphopentomutase enzyme that are bound with two ions (MN 502.B and MN 412.A) was visualised by using Pymol in the form of both cartoon and stick representation

339, and HIS-340, where the structural Mn ion functions to stabilise the overall structure of the phosphopentomutase enzyme.

After the structural superimposition process was performed, the computed Root Mean Square Deviation (RMSD) between the structure of *S. agalactiae* phosphopentomutase and *B. cereus* phosphopentomutase (PDB ID: 3UN2; chain A only) is 0.860 angstroms. Whereas the computed RMSD between the structure of *S. agalactiae* phosphopentomutase and *B. cereus* ATCC 14579 phosphopentomutase (PDB ID: 3M8Z; chain A only) is 0.890 angstroms. On the other hand, the computed RMSD between the structure of *S. agalactiae* phosphopentomutase and *S. mutans* phosphopentomutase (PDB ID: 3M7V; chain B only) is 0.689 angstroms. Among the three homologues, it can be observed that *S. mutans* phosphopentomutase is the most well-superimposed structure since its computed RMSD value is the lowest and its predicted e-value is zero. This is because the lower the RMSD value, the higher the percentage of structural similarity between the query *S. agalactiae* phosphopentomutase and its homologue (Meng *et al*., 2006).

Overall, based on Figure 5, it can be observed that all the cofactor binding residues of *S. agalactiae* phosphopentomutase and its homologues are located at similar regions whereby they are pointing at similar positions after the structural superimposition process was performed. Therefore, this further verifies the exact location of the cofactor binding site of *S. agalactiae* phosphopentomutase; thus, showing that the cofactor binding residues of *S. agalactiae* phosphopentomutase are conserved among its homologues in terms of location and functionality.

Molecular Docking between S. agalactiae Phosphopentomutase and MNPs

The AutoDock4 results of molecular docking between the eight MNPs and *S. agalactiae* phosphopentomutase are plotted in Table 6. It can be observed that the binding energy values of the eight different MNPs with compound ID numbers of CMNPD30311, CMNPD30314, CMNPD30308, CMNPD30312, CMNPD30307, CMNPD30310, CMNPD30313, and CMNPD30309 are -8.73, -8.69, -8.45, -8.33, -8.32, -8.04, -7.33, and -7.09, respectively. Generally, ligands with low binding energy possess higher binding affinity towards the receptor (Salha *et al*., 2021) since the ligand only requires low energy to bind to the receptor. Also, the low binding energy of the ligand indicates higher stability of the receptor-ligand complex (Joshi *et al*., 2021) since the ligand fits well into the binding site of the receptor complementarily in terms of its shape and conformation.

In terms of hydrogen bond interaction between the *S. agalactiae* phosphopentomutase and MNPs, it can be observed that CMNPD30313 forms the highest number of hydrogen bonds with the receptor, which is seven in this case. Meanwhile, CMNPD30311,

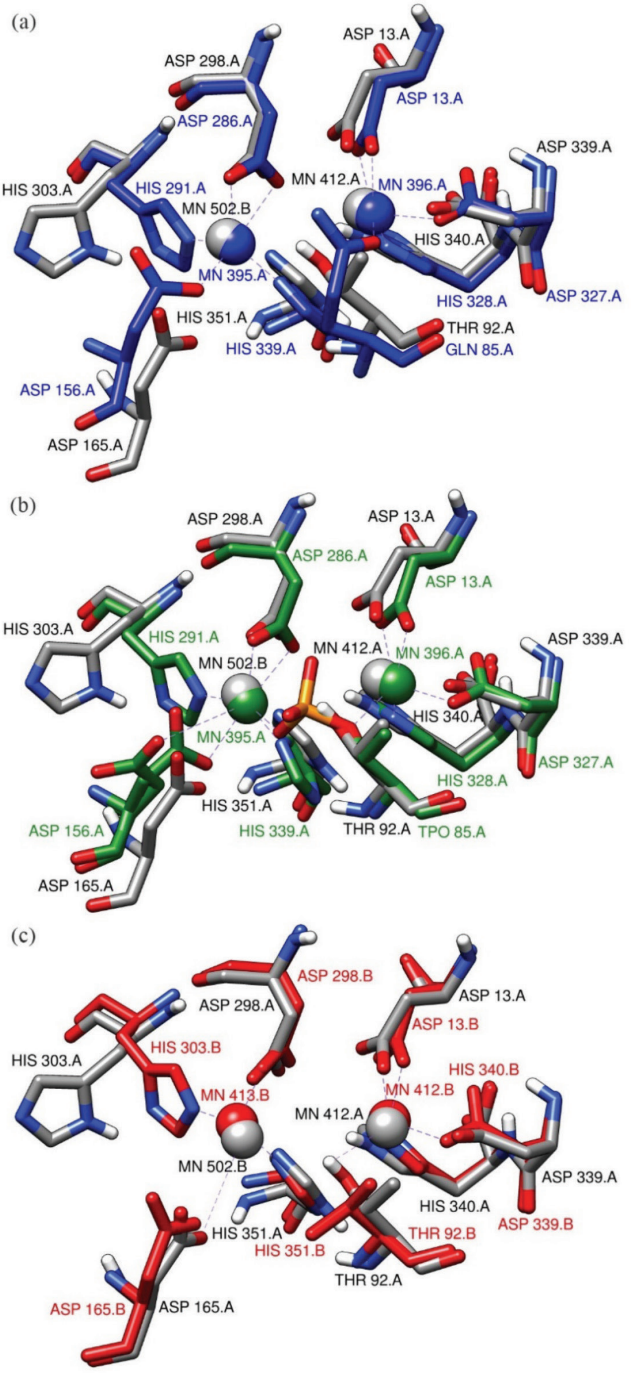

Figure 5: Structural superimposition between the cofactor binding sites of (a) *S. agalactiae* phosphopentomutase (coloured in grey) and *B. cereus* phosphopentomutase (PDB ID: 3UN2; chain A only; coloured in blue); (b) *S. agalactiae* phosphopentomutase and *B. cereus* ATCC 14579 phosphopentomutase (PDB ID: 3M8Z; chain A only; coloured in green); and (c) *S. agalactiae* phosphopentomutase and *S. mutans* phosphopentomutase (PDB ID: 3M7V; chain B only; coloured in red) to compare the cofactor binding sites

Table 6: Lists of binding energy values and total number of hydrogen bonds formed for every single best conformation of MNP that have been ranked in the increasing order of binding energy value

MNP Compounds	Compound ID Number	Binding Energy (kcal/mol)	No. of Hydrogen Bonds Formed
16-O-propionyl-16-O-deacetylhelvolic acid	CMNPD30311	-8.73	5
24-epi-6ß,16ß-diacetoxy-25-hydroxy-3,7-dioxo-29-nordammara-1,17(20)-diene-21,24-lactone	CMNPD30314	-8.69	5
6-O-propionyl-6,16-O-dideacetylhelvolic acid 21,16-lactone	CMNPD30308	-8.45	2
6-O-propionyl-6-O-deacetylhelvolic acid	CMNPD30312	-8.33	5
16-O-deacetylhelvolic acid 21,16-lactone	CMNPD30307	-8.32	3
1,2-dihydro-16-O-deacetylhelvolic acid 21,16-lactone	CMNPD30310	-8.04	2
6ß,16ß-diacetoxy-25-hydroxy-3,7-dioxo-29-nordammara-1,17(20)-dien-21,24-lactone	CMNPD30313	-7.33	7
1,2-dihydro-6,16-O-dideacetylhelvolic acid 21,16-lactone	CMNPD30309	-7.09	3

CMNPD30314, and CMNPD30312 each form five hydrogen bonds with the receptor, whereas CMNPD30307 and CMNPD30309 each form three hydrogen bonds with the receptor. On the other hand, CMNPD30308 and CMNPD30310 each only form two hydrogen bonds with the receptor. The greater the number of non-covalent bonded interactions (Sagaama *et al*., 2021), the higher the stability of the receptor-ligand complex.

Pharmacokinetic Assessment of MNPs

The pharmacokinetics and drug-likeness properties of the eight MNPs were evaluated using the SwissADME server, focusing on Lipinski's rule compliance. The result of the pharmacokinetic assessment is tabulated as shown in Table 7. Among the compounds, CMNPD30309 emerged as the most promising candidate, fully adhering to Lipinski's rule with an ideal molecular weight of 468.62 g/mol (Santos *et al*., 2016). This property is crucial for efficient membrane permeability and metabolism (Chagas *et al*., 2018). All MNPs demonstrated appropriate structural flexibility with less than 10 rotatable bonds, which is important for membrane permeability and stability (Damião *et al*., 2014; Maple *et al*., 2019).

The MNPs exhibited suitable lipophilicity with acceptable numbers of hydrogen bond acceptors and donors, essential for membrane permeability and metabolic stability (Abraham *et al*., 2002; Pajouhesh & Lenz, 2005). Most MNPs had favourable partition coefficient (Log $P_{o/w}$) values between three and five, except CMNPD30308, indicating good solubility and absorption potential (Mannhold *et al*., 2009; Das *et al*., 2022). These characteristics suggest that the majority of MNPs have the potential to cross biological membranes effectively and maintain stability in physiological conditions.

Table 7: List of MNPs with their respective molecular weight, number of rotatable bonds, number of hydrogen bond acceptors, number of hydrogen bond donors, consensus Log $P_{o/w}$, GI absorption, and bioavailability scores

MNPs	Molecular Weight (g/mol)	No. of Rotatable Bonds	No. of H-bond Acceptors	No. of H-bond Donors	Log $P_{o/w}$	GI Absorption	Bioavailability Scores
CMNPD30311	582.72	9	8	1	4.94	Low	0.56
CMNPD30314	584.70	5	9	1	3.69	Low	0.55
CMNPD30308	522.67	6	6	0	5.07	High	0.55
CMNPD30312	582.72	9	8	1	4.84	Low	0.56
CMNPD30307	508.65	5	6	0	4.79	High	0.55
CMNPD30310	510.66	5	6	0	4.90	High	0.55
CMNPD30313	584.70	5	9	1	3.66	Low	0.55
CMNPD30309	468.62	3	5	1	4.43	High	0.55

However, the assessment revealed some limitations among the compounds. Four MNPs (CMNPD30311, CMNPD30312, CMNPD30313, and CMNPD30314) showed poor GI absorption, which could impact their oral bioavailability. The bioavailability scores for all MNPs ranged from 0.55 to 0.56, suggesting moderate systemic availability (Yalkowsky *et al*., 2006; O'Donovan *et al*., 2023). These findings highlight CMNPD30309 as the most suitable for oral drug development, emphasising the importance of considering multiple pharmacokinetic parameters in drug discovery, particularly for marine-derived compounds. Future research should focus on optimising the absorption properties of the less favourable MNPs and further investigating the potential of CMNPD30309 as a lead compound.

Virtual Screening and Selection of MNPs

Based on binding energy, pharmacokinetic properties, and 2D interactions with *S. agalactiae* phosphopentomutase, three MNPs emerged as the most promising candidates: 16-O-deacetyl helvolic acid 21,16-lactone (CMNPD30307), 1,2-dihydro-6,16-O-dideacetylhelvolic acid 21, 16-lactone (CMNPD30309), and 1,2-dihydro-16-O-deacetylhelvolic acid 21,16-lactone (CM NPD30310). These compounds exhibited low estimated free binding energies (-8.32, -7.09, and -8.04, respectively) with no unfavourable donor-donor interactions or bumps, indicating stable binding interactions and minimal steric clashes (Gholam *et al*., 2022). Additionally, they largely adhere to Lipinski's rule with a maximum of one violation allowed, suggesting potential for oral bioavailability.

The pharmacokinetic properties of these MNPs were evaluated using various parameters. CMNPD30309 fully complied with Lipinski's rule having a molecular weight below 500 g/mol (468.62 g/mol) while CMNPD30307 (508.65 g/mol) and CMNPD30310 (510.66 g/mol) slightly exceeded this threshold. All three compounds demonstrated favourable characteristics in terms of rotatable bonds (3-5), hydrogen bond acceptors (5-6), hydrogen bond donors (0-1), and consensus Log $P_{o/w}$ values (4.43-4.90). Importantly, they all exhibited high gastrointestinal (GI) absorption values and bioavailability scores of 0.55, indicating good potential for oral administration and systemic availability (Yalkowsky *et al*., 2006; O'Donovan *et al*., 2023).

The 2D and 3D binding interactions between these MNPs and *S. agalactiae* phosphopentomutase were visualised using the Biovia Discovery Studio server (Kemmish *et al*., 2017) and UCSF Chimera (Figure 6). CMNPD30307 and CMNPD30309 each formed

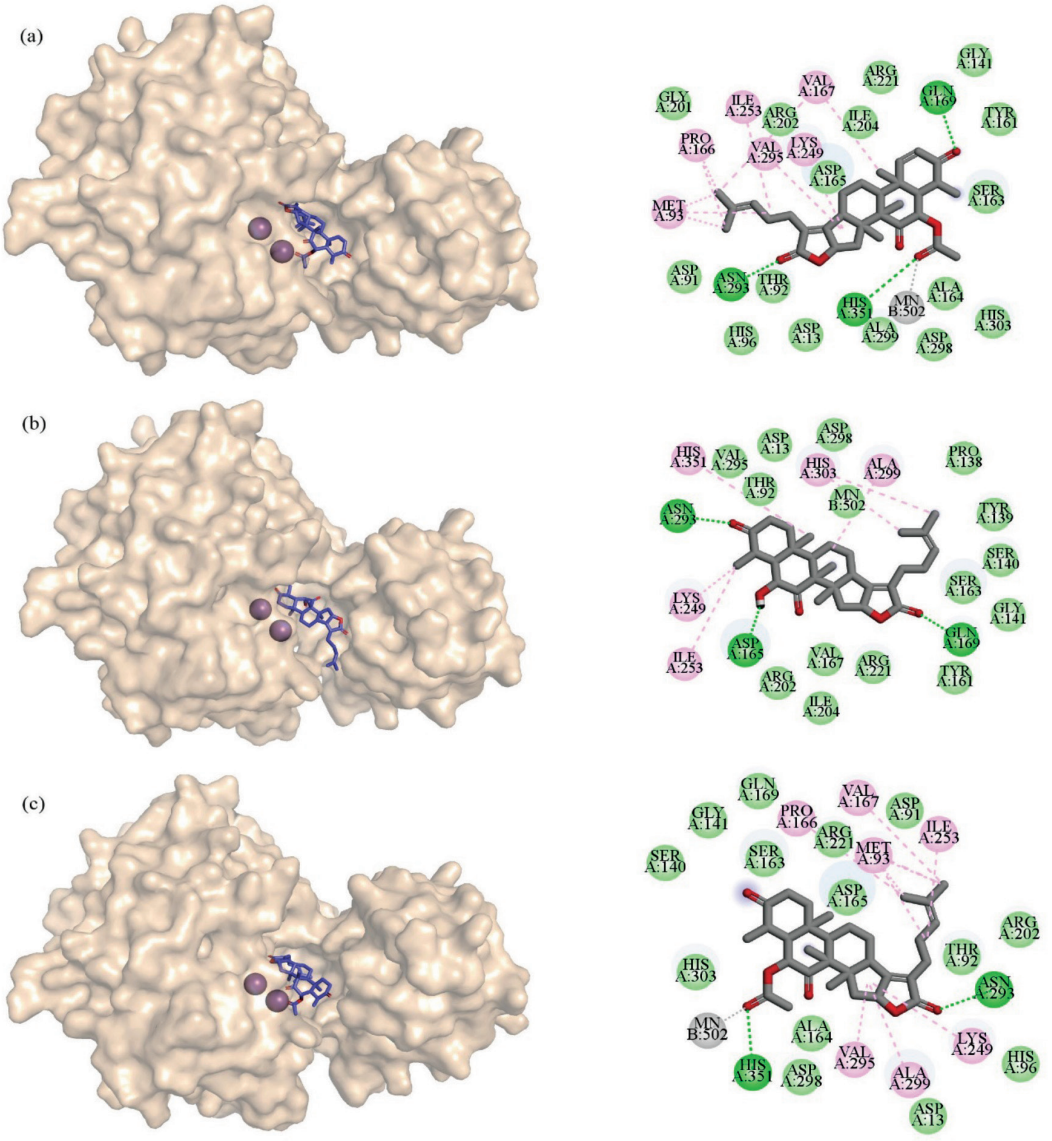

Figure 6: List of surface 3D and 2D representations of *S. agalactiae* phosphopentomutase that are bound with top three best MNPs, which are (a) CMNPD30307, (b) CMNPD30309, and (c) CMNPD30310 with their respective 2D interactions. Key amino acid residues that interact with the MNPs are represented in circles. Grey colour highlights the MNPs ligand in the form of stick representation; light grey colour indicates metal-acceptor interaction; green colour dotted line indicates conventional hydrogen bonds; light green colour dotted line indicates van der Waals interactions; and light purple colour indicates both alkyl and pi-alkyl interactions. Green colour amino acids represent conventional hydrogen bond interactions and light green colour amino acids without interactions represent van der Waals interactions. The blue halo that surrounds the interacting residues represents the solvent-accessible surface that is proportional to its diameter

three hydrogen bonds with the receptor while CMNPD30310 formed two. Specifically, CMNPD30307 interacted with GLN-169, ASN-293, and HIS-351; CMNPD30309 with ASP-165, GLN-169, and ASN-293; and CMNPD30310 with ASN-293 and HIS-351. Additionally, CMNPD30307 and CMNPD30310 demonstrated metal-acceptor interactions with MN 502.B of the receptor while CMNPD30309 exhibited weak van der Waals interactions with the same residue.

In conclusion, these three MNPs (CMNPD30307, CMNPD30309, and CMNPD30310) demonstrate promising characteristics as potential inhibitors of *S. agalactiae* phosphopentomutase. Their low binding energies, favourable pharmacokinetic properties, and specific interactions with the target protein suggest they could be effective and bioavailable as oral medications. Further in vitro and in vivo studies are warranted to validate these computational predictions and explore their potential as novel antibacterial agents.

Conclusions

This study demonstrates the efficacy of bioinformatic tools in sustainable drug discovery, specifically in identifying potential inhibitors of *S. agalactiae* phosphopentomutase. Three MNPs, namely CMNPD30307, CMNPD30309, and CMNPD30310 emerged as promising candidates, exhibiting favorable characteristics including compliance with Lipinski's rule, low binding energy, high binding affinity, high GI absorption, and high bioavailability scores. These compounds show potential for blocking D-ribose-5-phosphate synthesis; thus, inhibiting the nucleic acid biosynthesis process of *S. agalactiae*. While in vitro and in vivo testing remains necessary for validation, these findings highlight the potential of MNPs as novel antibiotics against *S. agalactiae* infections, aligning with sustainable approaches to science and management. Future research should focus on experimental validation of these compounds and implement sustainable bioprospecting approaches such as ethical sourcing, biodiversity conservation, and green technologies. This approach advances the antibacterial drug discovery process, ensures the long-term health and sustainability of aquatic ecosystems, and embodying the principles of sustainable science and management in marine bioresource utilisation.

Acknowledgements

This work was supported by Universiti Malaysia Terengganu through the Talent and Publication Enhancement Research Grant (UMT/TAPE-RG/2020/55298) and the Ministry of Higher Education (MoHE) Malaysia through the Fundamental Research Grants Scheme (FGRS/1/2021/STG01/UMT/02/2).

Conflicts of Interest Statement

The authors declare that they have no conflict of interest.

References

Abdullah, O. M., Elhadidy, G. S., Khamiss, R. E., Taha, O. T., & Hamady, A. B. (2023). Identification of inducible clindamycin resistance gene in *Streptococcus agalactiae* isolates colonizing pregnant women in Suez Canal University Hospitals. *Microbes and Infectious Diseases*, *4*(4), 1246-1254. https://doi.org/10.21608/mid.2023.213246.1531

Abraham, M. H., Ibrahim, A., Zissimos, A. M., Zhao, Y. H., Comer, J., & Reynolds, D. P. (2002). Application of hydrogen bonding calculations in property-based drug design. *Drug Discovery Today*, *7*(20), 1056-1063. https://doi.org/10.1016/S1359-6446(02)02478-9

Aldana-Valenzuela, C., Rodriguez-López, A. M., & Guillén-Blancas, E. (2019). Fulminant early-onset neonatal sepsis due to *Streptococcus pneumoniae*: Case report and review of the literature. *Pediatric Reports*, *11*(1), 7953. https://doi.org/10.4081/pr.2019.7953

Asiamah, I., Obiri, S. A., Tamekloe, W., Armah, F. A., & Borquaye, L. S. (2023). Applications of molecular docking in natural products-based drug discovery. *Scientific African*, *20*, e01593. https://doi.org/10.1016/j.sciaf.2023.e01593

Benet, L. Z., Hosey, C. M., Ursu, O., & Oprea, T. I. (2016). BDDCS, the rule of 5 and drugability. *Advanced Drug Delivery Reviews*, *101*, 89-98. https://doi.org/10.1016/j.addr.2016.05.007

Bhattacharya, A., Tejero, R., & Montelione, G. T. (2007). Evaluating protein structures determined by structural genomics consortia. *Proteins: Structure*, *Function*, *and Bioinformatics*, *66*(4), 778-795. https://doi.org/10.1002/prot.21165

Bizarro, C. V., & Schuck, D. C. (2007). Purine and pyrimidine nucleotide metabolism in *Mollicutes*. *Genetics and Molecular Biology*, *30*, 190-201. https://doi.org/10.1590/S1415-47572007000200005

Caron, G., Digiesi, V., Solaro, S., & Ermondi, G. (2020). Flexibility in early drug discovery: Focus on the beyond-rule-of-5 chemical space. *Drug Discovery Today*, *25*(4), 621-627. https://doi.org/10.1016/j.drudis.2020.01.012

Casadevall, G., Duran, C., & Osuna, S. (2023). AlphaFold2 and deep learning for elucidating enzyme conformational flexibility and its application for design. *JACS Au*, *3*(6), 1554-1562. https://doi.org/10.1021/jacsau.3c00188

Chagas, C. M., Moss, S., & Alisaraie, L. (2018). Drug metabolites and their effects on the development of adverse reactions: Revisiting Lipinski's rule of five. *International Journal of Pharmaceutics*, *549*(1-2), 133-149. https://doi.org/10.1016/j.ijpharm.2018.07.046

Chen, P. (2005). Self-assembly of ionic-complementary peptides: A physicochemical viewpoint. *Colloids and Surfaces A: Physicochemical and Engineering Aspects*, *261*(1), 3-24. https://doi.org/10.1016/j.colsurfa.2004.12.048

Cicaloni, V., Costanti, F., Pasqui, A., Bianchini, M., Niccolai, N., & Bongini, P. (2022). A bioinformatics approach to investigate structural and non-structural proteins in human coronaviruses. *Frontiers in Genetics*, *13*. https://doi.org/10.3389/fgene.2022.891418

Colovos, C., & Yeates, T. O. (1993). Verification of protein structures: Patterns of nonbonded atomic interactions. *Protein Science: A Publication of the Protein Society*, *2*(9), 1511-1519. https://doi.org/10.1002/pro.5560020916

Daina, A., Michielin, O., & Zoete, V. (2017). SwissADME: A free web tool to evaluate pharmacokinetics, drug-likeness and medicinal chemistry friendliness of small molecules. *Scientific Reports*, *7*(1), 42717. https://doi.org/10.1038/srep42717

Damião, M. C. F. C. B., Pasqualoto, K. F. M., Polli, M. C., & Filho, R. P. (2014). To be drug or prodrug: Structure-property exploratory approach regarding oral bioavailability. *Journal of Pharmacy & Pharmaceutical Sciences*, *17*(4). https://doi.org/10.18433/J3BS4H

Das, B., Baidya, A. T. K., Mathew, A. T., Yadav, A. K., & Kumar, R. (2022). Structural modification aimed for improving solubility of lead compounds in early phase drug discovery. *Bioorganic and Medicinal Chemistry*, *56*, 116614. https://doi.org/10.1016/j.bmc.2022.116614

Deng, L., Li, Y., Geng, Y., Zheng, L., Rehman, T., Zhao, R., Wang, K., OuYang, P., Chen, D., Huang, X., & He, C. (2019). Molecular serotyping and antimicrobial susceptibility of *Streptococcus agalactiae* isolated from fish in China. *Aquaculture*, *510*, 84-89. https://doi.org/10.1016/j.aquaculture.2019.05.046

Deng, Y., Liu, Y., Li, J., Wang, X., He, S., Yan, X., Shi, Y., Zhang, W., & Ding, L. (2022).

Marine natural products and their synthetic analogs as promising antibiofilm agents for antibiotics discovery and development. *European Journal of Medicinal Chemistry*, *239*, 114513. https://doi.org/10.1016/j.ejmech.2022.114513

Desai, D., Goh, K. G. K., Sullivan, M. J., Chattopadhyay, D., & Ulett, G. C. (2021). Hemolytic activity and biofilm-formation among clinical isolates of group B streptococcus causing acute urinary tract infection and asymptomatic bacteriuria. *International Journal of Medical Micro Biology*, *311*(6), 151520. https://doi.org/10.1016/j.ijmm.2021.151520

Doello, S., Neumann, N., & Forchhammer, K. (2022). Regulatory phosphorylation event of phosphoglucomutase 1 tunes its activity to regulate glycogen metabolism. *The FEBS Journal*, *289*(19), 6005-6020. https://doi.org/10.1111/febs.16471

Eisenberg, D., Luethy, R., & Bowie, J. (1997). VERIFY3D: Assessment of protein models with three-dimensional profiles. *Methods in Enzymology*, *277*, 396-404. https://doi.org/10.1016/S0076-6879(97)77022-8

Favero, L. M., Chideroli, R. T., Ferrari, N. A., Azevedo, V. A. D. C., Tiwari, S., Lopera-Barrero, N. M., & Pereira, U. de P. (2020). *In silico* prediction of new drug candidates against the multidrug-resistant and potentially zoonotic fish pathogen serotype III *Streptococcus agalactiae*. *Frontiers in Genetics*, *11*. https://doi.org/10.3389/fgene.2020.01024

Forli, S., Huey, R., Pique, M. E., Sanner, M., Goodsell, D. S., & Olson, A. J. (2016). Computational protein-ligand docking and virtual drug screening with the AutoDock suite. *Nature Protocols*, *11*(5), 905-919. https://doi.org/10.1038/nprot.2016.051

Gholam, G. M., Firdausy, I. A., Artika, I. M., Abdillah, R. M., & Firmansyah, R. P. (2022). Molecular docking: Bioactive compounds of *Mimosa pudica* as an inhibitor of *Candida albicans* Sap 3 (p. 2022.09.06.506736). *bioRxiv*. https://doi.org/10.1101/2022.09.06.506736

Ghosal, M., Rakhshit, T., Bhattacharya, S., Bhattacharyya, S., Satpati, P., Senapati, D., 2023. E-protein protonation titration-induced single particle chemical force spectroscopy for microscopic understanding and pI estimation of infectious DENV (p. 2023.03.30.534862). *bioRxiv*. https://doi.org/10.1101/2023.03.30.534862

Giesen, K. J. D. V., Thompson, M. J., Meng, Q., & Lovelock, S. L. (2023). Biocatalytic synthesis of antiviral nucleosides, cyclic dinucleotides, and oligonucleotide therapies. *JACS Au*, *3*(1), 13-24. https://doi.org/10.1021/jacsau.2c00481

Hussain, H., Xiao, J., Ali, A., R. Green, I., & Westermann, B. (2023). Unusually cyclized triterpenoids: Occurrence, biosynthesis and chemical synthesis. *Natural Product Reports*, *40*(2), 412-451. https://doi.org/10.1039/D2NP00033D

Hussein, M. E., Mohamed, O. G., El-Fishawy, A. M., El-Askary, H. I., El-Senousy, A. S., El-Beih, A. A., Nossier, E. S., Naglah, A. M., Almehizia, A. A., Tripathi, A., & Hamed, A. A. (2022). Identification of antibacterial metabolites from endophytic fungus *Aspergillus fumigatus*, isolated from *Albizia lucidior* leaves (*Fabaceae*), utilizing metabolomic and molecular docking techniques. *Molecules*, *27*(3), 1117. https://doi.org/10.3390/molecules27031117

Jha, P., Chaturvedi, S., Bhat, R., Jain, N., & Mishra, A. K. (2022). Insights of ligand binding in modeled h5-HT1A receptor: Homology modeling, docking, MM-GBSA, screening and molecular dynamics. *Journal of Biomolecular Structure and Dynamics*, *40*(22), 11625-011637. https://doi.org/10.1080/07391102.2021.1961865

Joshi, T., Joshi, T., Sharma, P., Chandra, S., & Pande, V. (2021). Molecular docking and molecular dynamics simulation approach to screen natural compounds for inhibition of *Xanthomonas oryzae* pv. Oryzae by

targeting peptide deformylase. *Journal of Biomolecular Structure and Dynamics*, *39*(3), 823-840. https://doi.org/10.1080/07391102.2020.1719200

Joyce, L. R., & Doran, K. S. (2023). Gram-positive bacterial membrane lipids at the host–pathogen interface. *PLOS Pathogens*, *19*(1), e1011026. https://doi.org/10.1371/journal.ppat.1011026

Jumper, J., Evans, R., Pritzel, A., Green, T., Figurnov, M., Ronneberger, O., Tunyasuvunakool, K., Bates, R., Žídek, A., Potapenko, A., Bridgland, A., Meyer, C., Kohl, S. A. A., Ballard, A. J., Cowie, A., Romera-Paredes, B., Nikolov, S., Jain, R., Adler, J., Back, T., Petersen, S., Reiman, D., Clancy, E., Zielinski, M., Steinegger, M., Pacholska, M., Berghammer, T., Bodenstein, S., Silver, D., Vinyals, O., Senior, A.W., Kavukcuoglu, K., Kohli, P., & Hassabis, D. (2021). Highly accurate protein structure prediction with AlphaFold. *Nature*, *596*(7873), 7873. https://doi.org/10.1038/s41586-021-03819-2

Kazmi, S. R., Jun, R., Yu, M.-S., Jung, C., & Na, D. (2019). *In silico* approaches and tools for the prediction of drug metabolism and fate: A review. *Computers in Biology and Medicine*, *106*, 54-64. https://doi.org/10.1016/j.compbiomed.2019.01.008

Kemmish, H., Fasnacht, M., & Yan, L. (2017). Fully automated antibody structure prediction using BIOVIA tools: Validation study. *PLOS ONE*, *12*(5), e0177923. https://doi.org/10.1371/journal.pone.0177923

Kong, F.-D., Huang, X.-L., Ma, Q.-Y., Xie, Q.-Y., Wang, P., Chen, P.-W., Zhou, L.-M., Yuan, J.-Z., Dai, H.-F., Luo, D.-Q., & Zhao, Y.-X. (2018). Helvolic acid derivatives with antibacterial activities against *Streptococcus agalactiae* from the marine-derived fungus *Aspergillus fumigatus* HNMF0047. *Journal of Natural Products*, *81*(8), 1869-1876. https://doi.org/10.1021/acs.jnatprod.8b00382

Lacasse, M., Valentin, A.-S., Corvec, S., Bémer, P., Jolivet-Gougeon, A., Plouzeau, C., Tandé, D., Mereghetti, L., Bernard, L., Lartigue, M.-F., & on behalf of the CRIOGO Study Group. (2022). Genotypic characterization and biofilm production of Group B Streptococcus strains isolated from bone and joint infections. *Microbiology Spectrum*, *10*(2), e02329-21. https://doi.org/10.1128/spectrum.02329-21

Laskowski, R. A. (2022). PDBsum1: A standalone program for generating PDBsum analyses. *Protein Science*, *31*(12), e4473. https://doi.org/10.1002/pro.4473

Laskowski, R. A., Hutchinson, E. G., Michie, A. D., Wallace, A. C., Jones, M. L., & Thornton, J. M. (1997). PDBsum: A web-based database of summaries and analyses of all PDB structures. *Trends in Biochemical Sciences*, *22*(12), 488-490. https://doi.org/10.1016/S0968-0004(97)01140-7

Laskowski, R. A., MacArthur, M. W., & Thornton, J. M. (2012). PROCHECK: Validation of protein-structure coordinates. *International Tables for Crystallography*, 684-687. https://doi.org/10.1107/97809553602060000724

Lv, J., Hu, D., Gao, H., Kushiro, T., Awakawa, T., Chen, G.-D., Wang, C., Abe, I., & Yao, X.-S. (2017). Biosynthesis of helvolic acid and identification of an unusual C-4-demethylation process distinct from sterol biosynthesis. *Nature Communications*, *8*. https://doi.org/10.1038/s41467-017-01813-9

Lyu, C., Chen, T., Qiang, B., Liu, N., Wang, H., Zhang, L., & Liu, Z. (2021). CMNPD: A comprehensive marine natural products database towards facilitating drug discovery from the ocean. *Nucleic Acids Research*, *49*(D1), D509-D515. https://doi.org/10.1093/nar/gkaa763

Mannhold, R., Poda, G. I., Ostermann, C., & Tetko, I. V. (2009). Calculation of molecular lipophilicity: State-of-the-art and comparison of LogP methods on

more than 96,000 compounds. *Journal of Pharmaceutical Sciences*, *98*(3), 861-893. https://doi.org/10.1002/jps.21494

Maple, H. J., Clayden, N., Baron, A., Stacey, C., & Felix, R. (2019). Developing degraders: Principles and perspectives on design and chemical space. *MedChemComm*, *10*(10), 1755-1764. https://doi.org/10.1039/C9MD00272C

McLeod, A., Snipen, L., Naterstad, K., & Axelsson, L. (2011). Global transcriptome response in *Lactobacillus sakei* during growth on ribose. *BMC Microbiology*, *11*(1), 145. https://doi.org/10.1186/1471-2180-11-145

Meng, E. C., Pettersen, E. F., Couch, G. S., Huang, C. C., & Ferrin, T. E. (2006). Tools for integrated sequence-structure analysis with UCSF Chimera. *BMC Bioinformatics*, *7*(1), 339. https://doi.org/10.1186/1471-2105-7-339

Michael, T. N., Obagbuwa, I. C., Whata, A., & Madzima, K. (2023). A comparative modeling and comprehensive binding site analysis of the south african beta COVID-19 variant's spike protein structure. In M. Lahby, V. Pilloni, J. S. Banerjee, & M. Mahmud (Eds.), *Advanced AI and internet of health things for combating pandemics* (pp. 383-394). Springer International Publishing. https://doi.org/10.1007/978-3-031-28631-5_18

Miselli, F., Creti, R., Lugli, L., & Berardi, A. (2022). Group B Streptococcus late-onset neonatal disease: An update in management and prevention. *The Pediatric Infectious Disease Journal*, *41*(6), e263. https://doi.org/10.1097/INF.0000000000003517

Morris, G. M., Huey, R., Lindstrom, W., Sanner, M. F., Belew, R. K., Goodsell, D. S., & Olson, A. J. (2009). AutoDock4 and AutoDockTools4: Automated docking with selective receptor flexibility. *Journal of Computational Chemistry*, *30*(16), 2785-2791. https://doi.org/10.1002/jcc.21256

O' Donovan, D. H., De Fusco, C., Kuhnke, L., & Reichel, A. (2023). Trends in molecular properties, bioavailability, and permeability across the bayer compound collection. *Journal of Medicinal Chemistry*, *66*(4), 2347-2360. https://doi.org/10.1021/acs.jmedchem.2c01577

Osowole, A. A., Ekennia, A. C., Olubiyi, O. O., & Olagunju, M. (2017). Synthesis, spectral, thermal, antibacterial and molecular docking studies of some metal(II) complexes of 2-(1,3-benzothiazol-2-ylamino) naphthalene-1,4-dione. *Research on Chemical Intermediates*, *43*(4), 2565-2585. https://doi.org/10.1007/s11164-016-2780-8

Pajouhesh, H., & Lenz, G. R. (2005). Medicinal chemical properties of successful central nervous system drugs. *NeuroRx*, *2*(4), 541-553. https://doi.org/10.1602/neurorx.2.4.541

Panda, S., & Chandra, G. (2012). Physicochemical characterization and functional analysis of some snake venom toxin proteins and related non-toxin proteins of other chordates. *Bioinformation*, *8*(18), 891-896. https://doi.org/10.6026/97320630008891

Panosian, T. D., Nannemann, D. P., Watkins, G. R., Phelan, V. V., McDonald, W. H., Wadzinski, B. E., Bachmann, B. O., & Iverson, T. M. (2011). *Bacillus cereus* phosphopentomutase is an alkaline phosphatase family member that exhibits an altered entry point into the catalytic cycle. *The Journal of Biological Chemistry*, *286*(10), 8043-8054. https://doi.org/10.1074/jbc.M110.201350

Pereira, J., Simpkin, A. J., Hartmann, M. D., Rigden, D. J., Keegan, R. M., & Lupas, A. N. (2021). High-accuracy protein structure prediction in CASP14. *Proteins: Structure, Function, and Bioinformatics*, *89*(12), 1687-1699. https://doi.org/10.1002/prot.26171

Pettersen, E. F., Goddard, T. D., Huang, C. C., Meng, E. C., Couch, G. S., Croll, T. I., Morris, J. H., & Ferrin, T. E. (2021). UCSF ChimeraX: Structure visualization

for researchers, educators, and developers. *Protein Science*, *30*(1), 70-82. https://doi.org/10.1002/pro.3943

Phuoc, N. N., Linh, N. T. H., Crestani, C., & Zadoks, R. N. (2021). Effect of strain and enviromental conditions on the virulence of *Streptococcus agalactiae* (Group B Streptococcus; GBS) in red tilapia (*Oreochromis* sp.). *Aquaculture*, *534,* 736256. https://doi.org/10.1016/j.aquaculture.2020.736256

Qaiser, H., Saeed, M., Nerukh, D., & Ul-Haq, Z. (2021). Structural insight into TNF-α inhibitors through combining pharmacophore-based virtual screening and molecular dynamic simulation. *Journal of Biomolecular Structure & Dynamics*, *39*(16), 5920-5939. https://doi.org/10.1080/07391102.2020.1796794

Ratnaningsih, E., & Saepulloh, S. (2022). *In silico* analysis on the interaction of haloacid dehalogenase from *Bacillus cereus* IndB1 with 2-chloroalkanoic acid substrates. *The Scientific World Journal*, *2022*, e1579194. https://doi.org/10.1155/2022/1579194

Reddy, P. P., & Rao, U. M. V. (2020). Homology modeling and validation of bacterial superoxide dismutase enzyme, an antioxidant. *Research Journal of Pharmacy and Technology*, *13*(12), 6202-6205. https://doi.org/10.5958/0974-360X.2020.01081.1

Remko, M., Broer, R., & Remková, A. (2014). A comparative study of the molecular structure, lipophilicity, solubility, acidity, absorption and polar surface area of coumarinic anticoagulants and direct thrombin inhibitors. *RSC Advances*, *4*(16), 8072-8084. https://doi.org/10.1039/C3RA42347F

Rigden, D. J., Lamani, E., Mello, L. V., Littlejohn, J. E., & Jedrzejas, M. J. (2003). Insights into the catalytic mechanism of cofactor-independent phosphoglycerate mutase from X-ray crystallography, simulated dynamics and molecular modeling. *Journal of Molecular Biology*, *328*(4), 909-920. https://doi.org/10.1016/S0022-2836(03)00350-4

Robert, X., & Gouet, P. (2014). Deciphering key features in protein structures with the new ENDscript server. *Nucleic Acids Research*, *42*(W1), W320-W324. https://doi.org/10.1093/nar/gku316

Sagaama, A., Issaoui, N., Al-Dossary, O., Kazachenko, A. S., & Wojcik, Marek. J. (2021). Non covalent interactions and molecular docking studies on morphine compound. *Journal of King Saud University - Science*, *33*(8), 101606. https://doi.org/10.1016/j.jksus.2021.101606

Saito, Y., Watanabe, T., Kato, S., Kutsuzawa, D., Watanabe, K., & Watanabe, M. (2023). A case of recurrent infective endocarditis caused by *Streptococcus agalactiae*. *International Heart Journal*, *64*(1), 105-108. https://doi.org/10.1536/ihj.22-417

Salha, D., Andaç, M., & Denizli, A. (2021). Molecular docking of metal ion immobilized ligands to proteins in affinity chromatography. *Journal of Molecular Recognition*, *34*(2), e2875. https://doi.org/10.1002/jmr.2875

Santhoshkumar, R., & Yusuf, A. (2020). In silico structural modeling and analysis of physicochemical properties of curcumin synthase (CURS1, CURS2, and CURS3) proteins of *Curcuma longa*. *Journal of Genetic Engineering and Biotechnology*, *18*(1), 24. https://doi.org/10.1186/s43141-020-00041-x

Santos, G. B., Ganesan, A., & Emery, F. S. (2016). Oral administration of peptide-based drugs: Beyond Lipinski's rule. *ChemMedChem*, *11*(20), 2245-2251. https://doi.org/10.1002/cmdc.201600288

Schar, D., Zhang, Z., Pires, J., Vrancken, B., Suchard, M.A., Lemey, P., Ip, M., Gilbert, M., Van Boeckel, T. & Dellicour, S. (2023). Dispersal history and bidirectional human-fish host switching of invasive, hypervirulent *Streptococcus agalactiae* sequence type

283. *PLOS Global Public Health*, *3*(10), e0002454. https://doi.org/10.1371/journal.pgph.0002454

Sievers, F., Wilm, A., Dineen, D., Gibson, T. J., Karplus, K., Li, W., Lopez, R., McWilliam, H., Remmert, M., Söding, J., Thompson, J. D., & Higgins, D. G. (2011). Fast, scalable generation of high-quality protein multiple sequence alignments using Clustal Omega. *Molecular Systems Biology*, *7*(1), 539. https://doi.org/10.1038/msb.2011.75

Silva, H. D. D., & Winkelströter, L. K. (2019). Universal gestational screening for *Streptococcus agalactiae* colonization and neonatal infection - A systematic review and meta-analysis. *Journal of Infection and Public Health*, *12*(4), 479-481. https://doi.org/10.1016/j.jiph.2019.03.004

Sobolev, O. V., Afonine, P. V., Moriarty, N. W., Hekkelman, M. L., Joosten, R. P., Perrakis, A., & Adams, P. D. (2020). A global ramachandran score identifies protein structures with unlikely stereochemistry. *Structure*, *28*(11), 1249-1258.e2. https://doi.org/10.1016/j.str.2020.08.005

Syuhada, R., Zamri-Saad, M., Ina-Salwany, M. Y., Mustafa, M., Nasruddin, N. N., Desa, M. N. M., Nordin, S. A., Barkham, T., & Amal, M. N. A. (2020). Molecular characterization and pathogenicity of *Streptococcus agalactiae* serotypes Ia ST7 and III ST283 isolated from cultured red hybrid tilapia in Malaysia. *Aquaculture*, *515*, 734543. https://doi.org/10.1016/j.aquaculture.2019.734543

The UniProt Consortium. (2019). UniProt: A worldwide hub of protein knowledge. *Nucleic Acids Research*, *47*(D1), D506-D515. https://doi.org/10.1093/nar/gky1049

Tsalta-Mladenov, M. E., Dimitrova, V. M., Georgieva, D. K., & Andonova, S. P. (2022). *Streptococcus agalactiae* meningitis presented with cerebral infarction in adult patient – Clinical case and review. *Neurology India*, *70*(5), 2145. https://doi.org/10.4103/0028-3886.359190

Ugurel, O. M., Mutlu, O., Sariyer, E., Kocer, S., Ugurel, E., Inci, T. G., Ata, O., & Turgut-Balik, D. (2020). Evaluation of the potency of FDA-approved drugs on wild type and mutant SARS-CoV-2 helicase (Nsp13). *International Journal of Biological Macromolecules*, *163*, 1687-1696. https://doi.org/10.1016/j.ijbiomac.2020.09.138

Valasatava, Y., Rosato, A., Furnham, N., Thornton, J. M., & Andreini, C. (2018). To what extent do structural changes in catalytic metal sites affect enzyme function? *Journal of Inorganic Biochemistry*, *179*, 40-53. https://doi.org/10.1016/j.jinorgbio.2017.11.002

Walker, J. M. (Ed.). (2005). *The proteomics protocols handbook*. Humana Press. https://doi.org/10.1385/1592598900

Wang, J., Chitsaz, F., Derbyshire, M. K., Gonzales, N. R., Gwadz, M., Lu, S., Marchler, G. H., Song, J. S., Thanki, N., Yamashita, R. A., Yang, M., Zhang, D., Zheng, C., Lanczycki, C. J., & Marchler-Bauer, A. (2023). The conserved domain database in 2023. *Nucleic Acids Research*, *51*(D1), D384-D388. https://doi.org/10.1093/nar/gkac1096

Waring, M. J. (2009). Defining optimum lipophilicity and molecular weight ranges for drug candidates - Molecular weight dependent lower logD limits based on permeability. *Bioorganic & Medicinal Chemistry Letters*, *19*(10), 2844-2851. https://doi.org/10.1016/j.bmcl.2009.03.109

Wiederstein, M., & Sippl, M. J. (2007). ProSA-web: Interactive web service for the recognition of errors in three-dimensional structures of proteins. *Nucleic Acids Research*, *35*(suppl_2), W407-W410. https://doi.org/10.1093/nar/gkm290

Xu, D., Aihemaiti, Z., Cao, Y., Teng, C., & Li, X. (2016). Physicochemical stability, microrheological properties and microstructure of lutein emulsions stabilized by multilayer membranes consisting of whey protein isolate, flaxseed gum and chitosan.

Food Chemistry, *202*, 156-164. https://doi.org/10.1016/j.foodchem.2016.01.052

Yalkowsky, S. H., Johnson, J. L. H., Sanghvi, T., & Machatha, S. G. (2006). A 'rule of unity' for human intestinal absorption. *Pharmaceutical Research*, *23*(10), 2475-2481. https://doi.org/10.1007/s11095-006-9000-y

Yang, J.-M., & Tung, C.-H. (2006). Protein structure database search and evolutionary classification. *Nucleic Acids Research*, *34*(13), 3646-3659. https://doi.org/10.1093/nar/gkl395

Yoshida, M., Matsuda, K., Endo, K., Honda, A., Maki, H., Taoka, K., Masamoto, Y., Wakimoto, Y., Jubishi, D., Moriya, K., & Kurokawa, M. (2023). Toxic shock like syndrome caused by *Streptococcus agalactiae* bacteremia during treatment for multiple myeloma. *Journal of Infection and Chemotherapy*, *29*(4), 407-409. https://doi.org/10.1016/j.jiac.2022.12.001

Yuan, S., Chan, H. C. S., & Hu, Z. (2017). Using PyMOL as a platform for computational drug design. *WIREs Computational Molecular Science*, *7*(2), e1298. https://doi.org/10.1002/wcms.1298

Zheng, S., Xu, S., Wang, G., Tang, Q., Jiang, X., Li, Z., Xu, Y., Wang, R., & Lin, F. (2017). Proposed hydrogen-bonding index of donor or acceptor reflecting its intrinsic contribution to hydrogen-bonding strength. *Journal of Chemical Information and Modeling*, *57*(7), 1535-1547. https://doi.org/10.1021/acs.jcim.7b00022

Zohari, Z., Barkham, T., Mohamad Maswan, N., Chen, S.L., Muthanna, A., Lee, K.W., Mohd Desa, M.N., Azmai, M.N.A., Sither Joseph, N.M. & Amin-Nordin, S. (2023). Fish-associated *Streptococcus agalactiae* ST283: First human cases reported from Malaysia. *Journal of Medical Microbiology*, *72*(6), 001729. https://doi.org/10.1099/jmm.0.001729

Zuegg, J., & A. Cooper, M. (2012). Drug-likeness and increased hydrophobicity of commercially available compound libraries for drug screening. *Current Topics in Medicinal Chemistry*, *12*(14), 1500-1513. https://doi.org/10.2174/1568026128026524 66